

Opto-Electronic Advances

CN 51-1781/TN ISSN 2096-4579 (Print) ISSN 2097-3993 (Online)

Agile cavity ringdown spectroscopy enabled by moderate optical feedback to a quantum cascade laser

Qinxue Nie, Yibo Peng, Qiheng Chen, Ningwu Liu, Zhen Wang, Cheng Wang and Wei Ren

Citation: Nie QX, Peng YB, Chen QH, et al. Agile cavity ringdown spectroscopy enabled by moderate optical feedback to a quantum cascade laser. *Opto-Electron Adv* 7, 240077(2024).

<https://doi.org/10.29026/oea.2024.240077>

Received: 5 April 2024; Accepted: 6 August 2024; Published online: 20 September 2024

Related articles

A highly sensitive LITES sensor based on a multi-pass cell with dense spot pattern and a novel quartz tuning fork with low frequency

Yahui Liu, Shunda Qiao, Chao Fang, Ying He, Haiyue Sun, Jian Liu, Yufei Ma

Opto-Electronic Advances 2024 7, 230230 doi: [10.29026/oea.2024.230230](https://doi.org/10.29026/oea.2024.230230)

Sub-femtometer-resolution absolute spectroscopy with sweeping electro-optic combs

Bingxin Xu, Xinyu Fan, Shuai Wang, Zuyuan He

Opto-Electronic Advances 2022 5, 210023 doi: [10.29026/oea.2022.210023](https://doi.org/10.29026/oea.2022.210023)

More related article in Opto-Electronic Journals Group website 



<http://www.ojournal.org/oea>



 OE_Journal



 @OptoElectronAdv

DOI: [10.29026/oea.2024.240077](https://doi.org/10.29026/oea.2024.240077)

Agile cavity ringdown spectroscopy enabled by moderate optical feedback to a quantum cascade laser

Qinxue Nie¹, Yibo Peng², Qiheng Chen¹, Ningwu Liu¹, Zhen Wang¹,
Cheng Wang^{2*} and Wei Ren^{1*}

Cavity ringdown spectroscopy (CRDS), relying on measuring the decay time of photons inside a high-finesse optical cavity, offers an important analytical tool for chemistry, physics, environmental science, and biology. Through the reflection of a slight amount of phase-coherent light back to the laser source, the resonant optical feedback approach effectively couples the laser beam into the optical cavity and achieves a high signal-to-noise ratio. However, the need for active phase-locking mechanisms complicates the spectroscopic system, limiting its primarily laboratory-based use. Here, we report how passive optical feedback can be implemented in a quantum cascade laser (QCL) based CRDS system to address this issue. Without using any phase-locking loops, we reflect a moderate amount of light (−18.2 dB) to a continuous-wave QCL simply using a fixed flat mirror, narrowing the QCL linewidth from 1.2 MHz to 170 kHz and significantly increasing the laser-cavity coupling efficiency. To validate the method's feasibility and effectiveness, we measured the absorption line (P(18e), 2207.62 cm^{−1}) of N₂O in a Fabry–Perot cavity with a high finesse of ~52000 and an inter-mirror distance of 33 cm. This agile approach paves the way for revolutionizing existing analytical tools by offering compact and high-fidelity mid-infrared CRDS systems.

Keywords: cavity ringdown spectroscopy; optical feedback; quantum cascade laser; gas sensing

Nie QX, Peng YB, Chen QH et al. Agile cavity ringdown spectroscopy enabled by moderate optical feedback to a quantum cascade laser. *Opto-Electron Adv* 7, 240077 (2024).

Introduction

Cavity ringdown spectroscopy (CRDS), first invented for use with pulsed lasers¹ and subsequently adapted with continuous wave (CW) lasers², is a well-established spectroscopic technique renowned for its high sensitivity, resolution and accuracy^{3–6}. Different from direct absorption spectroscopy, which measures intensity attenuation^{7–10}, CRDS extracts the absorption information by measuring the ringdown time of photons in an optical cavity. This method employs a high-finesse opti-

cal cavity featuring two (or more) high-reflectivity mirrors separated by a certain distance (known as the cavity length), often used to increase the effective path length. As a result, the intracavity gas absorption is relevant to the ringdown time by the following equation²:

$$\alpha = \frac{1}{c} \left(\frac{1}{\tau} - \frac{1}{\tau_0} \right), \quad (1)$$

where α is the absorption coefficient of the gas inside the cavity, c is the speed of light, and τ_0 and τ are the

¹Department of Mechanical and Automation Engineering, The Chinese University of Hong Kong, Hong Kong SAR, China; ²School of Information Science and Technology, ShanghaiTech University, Shanghai 201210, China.

*Correspondence: W Ren, E-mail: renwei@mae.cuhk.edu.hk; C Wang, E-mail: wangcheng1@shanghaitech.edu.cn

Received: 5 April 2024; Accepted: 6 August 2024; Published online: 20 September 2024



Open Access This article is licensed under a Creative Commons Attribution 4.0 International License.

To view a copy of this license, visit <http://creativecommons.org/licenses/by/4.0/>.

© The Author(s) 2024. Published by Institute of Optics and Electronics, Chinese Academy of Sciences.

ringdown time of the cavity in vacuum and the presence of gas, respectively. Hence, CRDS is less sensitive to the intensity noise of the laser source compared to direct absorption spectroscopy. Over the past decades, CRDS has been well adapted to different types of lasers such as distributed feedback (DFB) diode lasers, external cavity diode lasers (ECDLs), quantum cascade lasers (QCLs) and interband cascade lasers (ICLs), for many spectroscopic and sensing applications^{11–16}.

High-sensitivity CRDS typically employs an optical cavity with a higher finesse or a larger inter-mirror distance. This inevitably reduces the transmission width of the cavity mode down to kHz level, significantly narrower than the linewidth of single-mode tunable lasers (i.e., DFB lasers), normally in the MHz range. Hence, only a fraction of the incident light can be effectively coupled into the optical cavity, leading to a noisy or distorted output signal^{17,18}. Effectively injecting the laser beam into the high-finesse cavity remains a challenge, which could be addressed by minimizing the laser linewidth^{19,20}.

Utilizing optical feedback, which reflects emitted light coherently back into the electromagnetic field inside the laser cavity, proves to be an effective approach for linewidth reduction or laser stabilization²¹. Here, we define the feedback rate (φ) as the ratio of the power returned to the laser to the original output power. Weak optical feedback ($\varphi < -30$ dB) can narrow the laser linewidth if the phase of the feedback light is precisely controlled to compensate for the phase mismatch caused by environmental variations²². In this scheme, a V-shape optical cavity is often used, where feedback comprises only the light leaked from the optical cavity. Thus, the cavity-filtered (narrow spectrum) phase-coherent light seeds the laser and narrows the emission spectrum²³. This resonant optical feedback approach, known as optical feedback (OF)-CRDS^{24–27}, has facilitated advancements in high-sensitivity and high-precision molecular spectroscopy. However, these spectroscopic systems require the feedback light to be precisely in phase with that inside the laser gain medium, necessitating an active phase-locking loop as a key element in OF-CRDS²⁸. This requirement renders the measurement system less flexible, less robust, and more costly.

Moderate ($\varphi = -30$ dB to -10 dB) or strong ($\varphi > -10$ dB) optical feedback is mostly avoided in optical systems due to the risk of coherence collapse, which easily destabilizes the laser and significantly broadens the laser linewidth^{21,29}. However, recent findings have challenged

this notion, particularly in the case of QCLs, which are unipolar devices cascading electrons to directly generate mid-infrared radiation. Due to their ultrashort carrier lifetime and small linewidth broadening factor³⁰, QCLs may exhibit high stability against moderate and strong optical feedback³¹. In fact, studies have shown that the linewidth of QCLs gradually becomes insensitive to the feedback phase with increasing feedback rates³². Hence, there is potential to develop an OF-CRDS system for molecular spectroscopy without using any phase-locking schemes.

In this work, we demonstrate an agile method for performing low-noise CRDS by employing moderate optical feedback into a QCL. Using a continuous-wave DFB-QCL with MHz-level linewidth and sub-mW emission power, we seed it with moderate optical feedback (-18.2 dB), leading to a significant linewidth narrowing without the need for any phase control. As a proof-of-concept experiment, we tune the QCL wavelength across a mid-infrared absorption line ($4.53\ \mu\text{m}$) of nitrous oxide (N_2O), which is diluted to ppb levels and filled in a high-finesse (~ 52000) optical cavity. Our method paves the way for the advancement of next-generation CRDS using QCLs or other semiconductor lasers, offering a straightforward configuration suitable for a wide range of spectroscopic applications.

Principle and experimental setup

Figure 1 depicts the schematic diagram of the proposed QCL-based CRDS with moderate optical feedback. The commercial QCL (Hamamatsu Photonics) undergoes polarization control via a half-wave plate (HWP), and is then split by an acousto-optic modulator (AOM): the zero-order (undiffracted) portion is used for optical feedback, while the first-order beam is sent to a Fabry–Perot cavity for cavity ringdown measurements. A gold-coated plane mirror reflects the zero-order beam to the QCL, wherein the optical feedback rate can be finely adjusted via a polarizing beamsplitter (PBS) and monitored by routing idle light to a power meter. It is worth noting that power monitoring is not required during actual ringdown measurements. The first-order diffraction is injected into the Fabry–Perot cavity, which comprises two plano-concave dielectric mirrors. Note that an optical isolator (34 dB isolation) is used to block the light returned from the optical cavity. The two mirrors are separated by 33 cm, and the inter-mirror distance can be dithered via a piezoelectric actuator (PZT) attached to

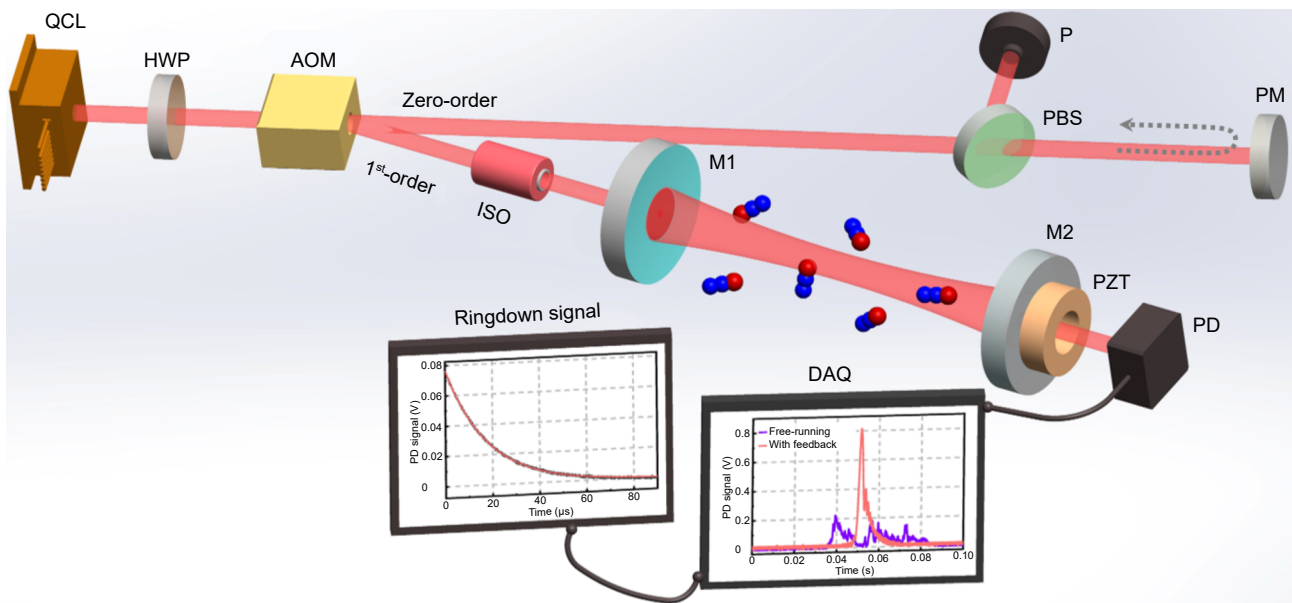


Fig. 1 | Principle of the agile CRDS with moderate optical feedback to a QCL. HWP: half-wave plate; AOM: acousto-optic modulator; PBS: polarizing beamsplitter; PM: plane mirror; P: power meter; ISO: optical isolator; M1, M2: cavity mirrors; PZT: piezoelectric actuator; PD: photodetector; DAQ: data acquisition card.

the rear mirror of the cavity. To ensure ringdown events occur at each laser frequency, the longitudinal mode of the cavity is swept using the PZT. The cavity output is captured by a mercury cadmium telluride (MCT) photodetector with a bandwidth of 10 MHz. A segment of the photodetector signal is sent to a comparator circuit, which triggers the AOM driver to interrupt the first-order beam and synchronizes the data acquisition card for recording the ringdown signal. Hence, the entire OF-CRDS system is established without relying on any phase-locking loop, which significantly reduces the configuration complexity.

Results and discussion

Characterization of QCL linewidth and ringdown signal

We first quantitatively investigated the effect of linewidth reduction using the passive optical feedback approach. To assess the QCL linewidth³², the optical cavity described in Fig. 1 was replaced by a 1-cm gas cell filled with 15-Torr pure CO to convert laser frequency noise into intensity noise. As shown in Fig. 2(a), the AOM is turned on to ensure the first-order beam consistently enters the reference gas cell containing carbon monoxide (CO). A typical transmission signal is illustrated in Fig. 2(b), with the blue side of the CO absorption line at 2209.5 cm^{-1} serving as a frequency discriminator. This gives a frequency-intensity conversion factor of 45.2

mV/MHz in a linear frequency span of approximately 150 MHz; further details are available in Supplementary information Section 1. As shown in Fig. 2(c), the free-running QCL exhibits a linewidth of about 1.2 MHz with a 0.2-ms observation time, decreasing to a minimum of 170 kHz at a feedback rate of -16.8 dB. However, increasing the feedback rate beyond this point does not further reduce the linewidth; instead, it results in multi-mode emission when the feedback rate exceeds -11.6 dB.

We then directed the first-order QCL beam into the optical cavity, as shown in Fig. 1, to explore the cavity output at different levels of optical feedback. To initiate laser-cavity resonance, the cavity length was swept every 0.1 s using a 5-Hz triangle waveform. Figure 3 compares cavity-transmitted signals of the QCL with different optical feedback rates alongside the signal of the free-running QCL, spanning two periods; four cavity-transmitted signals are shown in the same figure. It is evident that the cavity-transmitted signal exhibits significant fluctuations when the QCL is operating in free-running mode or with weak optical feedback (-49 dB). In contrast, the cavity-transmitted signal shows greater consistency with moderate optical feedback (-18.2 dB and -14.8 dB), displaying an expected asymmetric profile characterized by a rapid build-up phase followed by a gradual decay³³. More importantly, the signal amplitude reaches a large value of 0.8 V. In the following cavity ringdown measurements, we used the feedback rate of -18.2 dB,

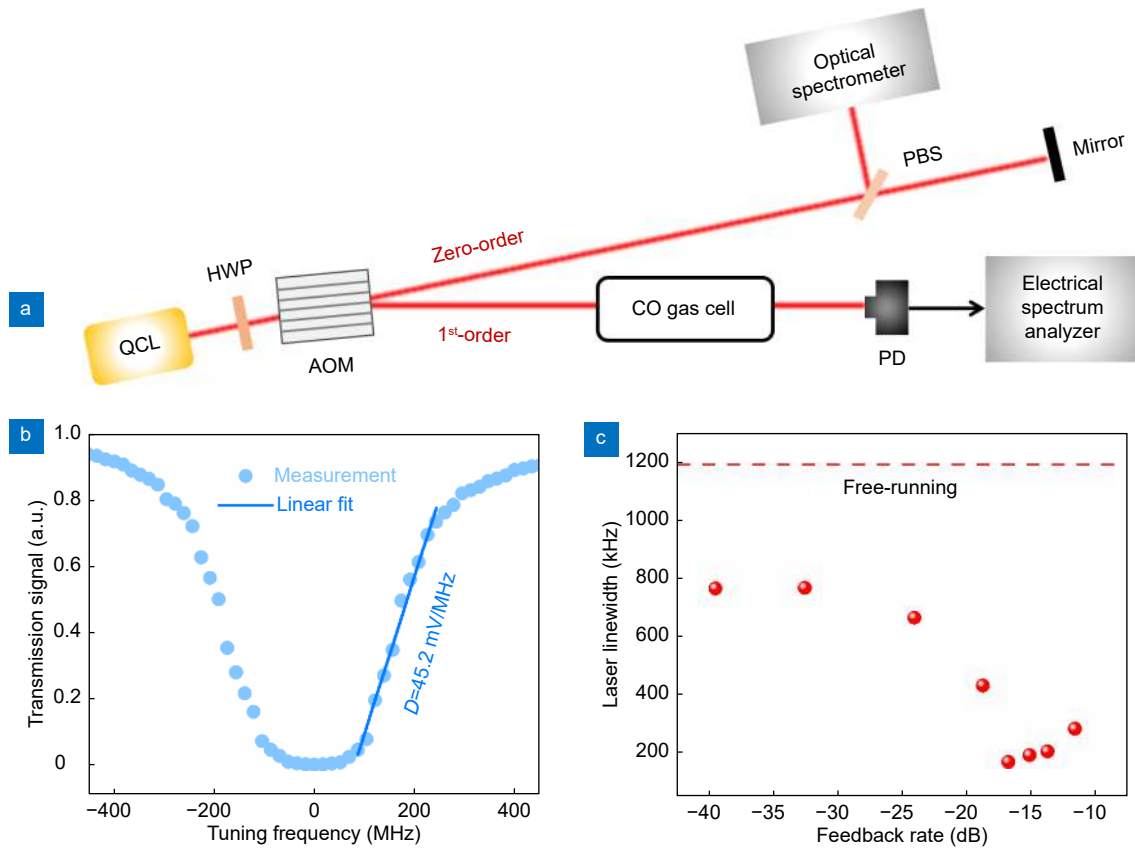


Fig. 2 | Characterization of QCL linewidth. (a) Experimental setup. The absorption line of CO sealed in a gas cell (15 Torr) is used as a frequency discriminator. (b) Typical transmission signal of the QCL through the CO reference cell. (c) Variation of QCL linewidth with the feedback rate. The dashed line indicates the linewidth of the free-running QCL.

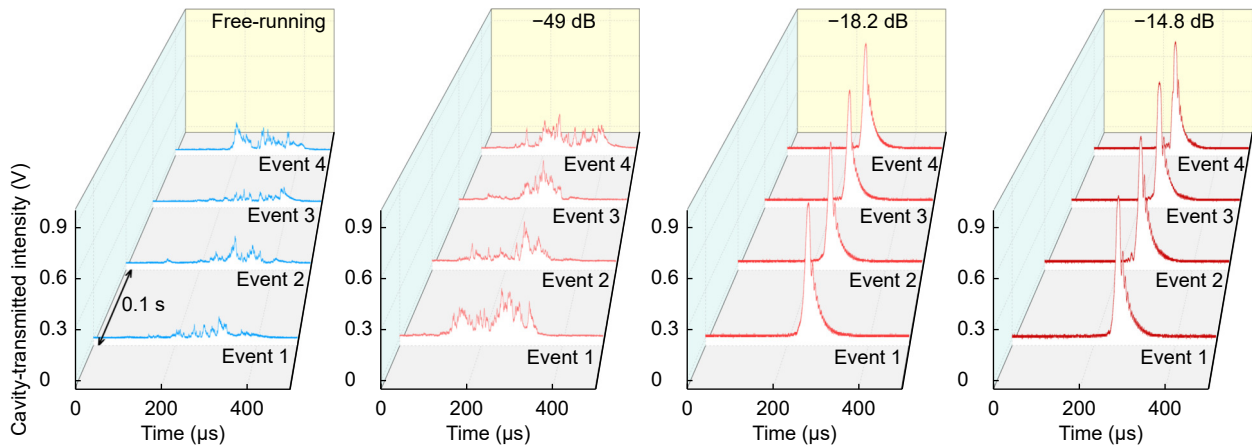


Fig. 3 | Comparison of the cavity-transmitted signals with different levels of optical feedback. Four ringdown events obtained by scanning the cavity length with a triangle waveform (5 Hz) are shown in each figure. The QCL is operating either at the free-running state or with optical feedback (from -49 dB to -14.8 dB).

considering the relatively favorable signal-to-noise ratio (SNR).

To showcase the effectiveness of the proposed method, we reduced the QCL power to a very low level of 0.4 mW by using a lower injection current to investigate the capability of observing the ringdown events under low-pow-

er conditions. Upon the photodetector signal reaching the threshold voltage (i.e., 80 mV), the incident laser was promptly interrupted by the AOM to initiate an intra-cavity ringdown. Figure 4(a) illustrates a representative ringdown event, which can be well-fitted by an exponential function. The ringdown time constant is determined

to be 18.25 μs for the cavity in a vacuum (see Supplementary information Section 2), corresponding to a reflectivity of 99.994% for the two identical cavity mirrors. The measurement is in good agreement with the nominal reflectivity of 99.992%, provided by the manufacturer (LohnStar Optics Inc.). The methods of determining the ringdown time and the mirror reflectivity are provided in Supplementary information Section 2. Given the known mirror reflectivity and cavity length, the linewidth of the optical cavity is determined to be 8.7 kHz. The system's stability was also evaluated by continuously recording over 300 ringdown events (Fig. 4(c)) and calculating the Allan deviation of the cavity ringdown time. As depicted in Fig. 4(b), the precision of the ringdown time measurement can be improved to 0.02 μs after averaging 20 ringdown events.

Spectrometer performance

The QCL-based CRDS system is characterized by measuring the absorption line of N_2O . Over the spectral range covered by the DFB-QCL (2207-2212 cm^{-1}), we aim to exploit the strong N_2O absorption line, P(18e), centered at 2207.62 cm^{-1} . This particular absorption line exhibits minimal spectral interference from other atmospheric molecules, which is illustrated in Supplementary information Section 3 through spectral simulation. To demonstrate the high sensitivity and reliability of the developed CRDS system, we conducted measurements of

ppb-level N_2O mixtures by diluting a $\text{N}_2\text{O}/\text{N}_2$ cylinder with a certified volume fraction of 1.2 ppm N_2O . However, we found that the ultrahigh-purity (> 99.999%) N_2 gas cylinder used for dilution contains about 74 ppb N_2O and 85 ppb CO as impurities (see Supplementary information Section 4). A similar discovery of impurities in ultrahigh-purity N_2 gas cylinders has also been reported previously³⁴. To prepare the ppb-level N_2O gas samples, we diluted the certified 1.2 ppm N_2O with high-purity helium (He) (> 99.995%) using a high-precision automatic gas mixing system (LaSense Technology Ltd.). The uncertainties associated with the nominal concentrations are mainly attributed to the accuracy of the mass flow controllers ($\pm 1\%$). It should be noted that N_2O has a tendency for surface adsorption. Hence, all subsequent experiments were conducted under flowing conditions with a volume flow rate of 2 L/min to ensure a more accurate nominal N_2O concentration.

Figure 5(a) depicts the typical absorption spectrum of 10 ppb N_2O measured at atmospheric pressure; the absorption coefficient was derived from the ringdown time using Eq. (1). Each data point in the spectrum was acquired by scanning the laser current in a step-wise manner with a step size of 0.5 mA, characterized to align with the cavity's free spectral range (FSR). The absorption coefficient at each laser frequency was determined by taking 300 averages of the ringdown time measurements. The measured spectrum can be well fitted by the

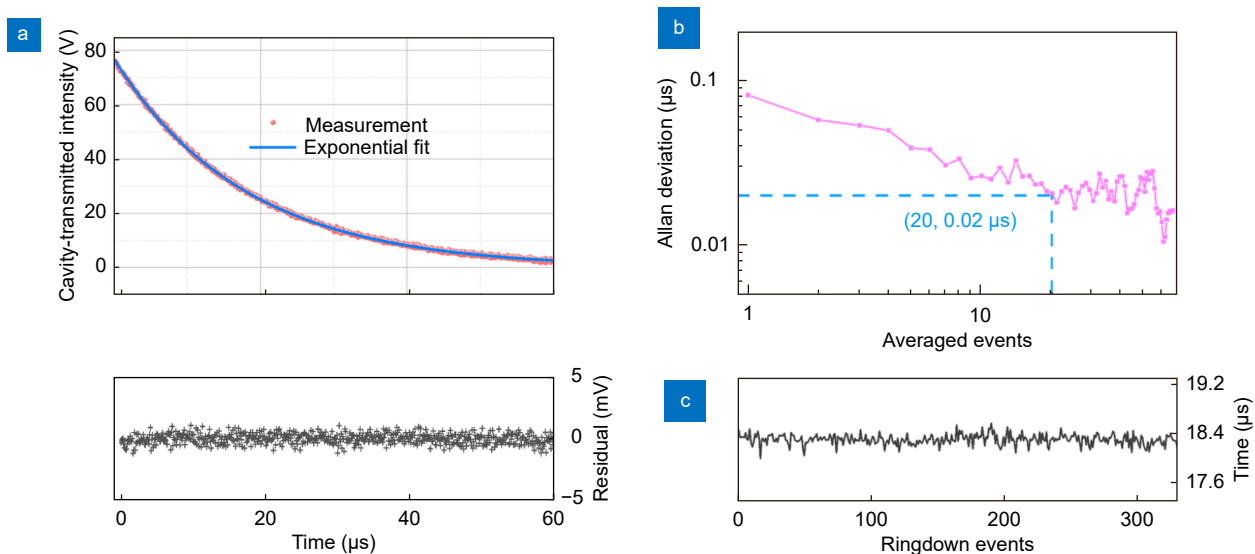


Fig. 4 | Cavity ringdown measurement with a feedback rate of -18.2 dB. The cavity is in a vacuum. (a) Characterization of a single cavity ringdown event with an incident optical power of 0.4 mW. The residual between the measurement and exponential fit is plotted in the bottom panel, and the SNR of the ringdown signal is 162. **(b)** Allan deviation analysis of the ringdown time measurement. **(c)** Continuous measurement of more than 300 ringdown events.

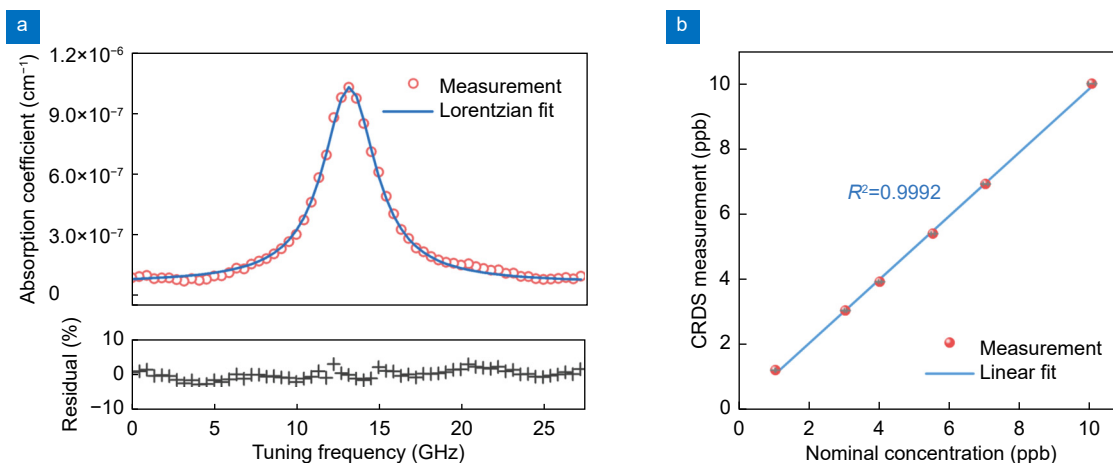


Fig. 5 | High-resolution and high-sensitivity molecular spectroscopy of trace amount of N₂O. (a) Measured absorption spectrum of 10 ppb N₂O. The residual of the spectral fitting by the Lorentzian function is plotted in the bottom panel. (b) Comparison of the CRDS measurements with the nominal concentrations of N₂O (1–10 ppb). The horizontal error bar represents the uncertainty in the nominal gas concentration, while the vertical error bar (too small to be visible) represents the 1- σ standard deviation of 300 CRDS measurements.

Lorentzian function, with a relative fitting residual within 3%, as shown in the bottom panel of Fig. 5(a). The relative residual is obtained by dividing the fitting residual by the peak absorbance. The SNR of the measured spectrum is evaluated to be 75, which is obtained by dividing the peak absorbance by the 1- σ standard deviation of the absolute fitting residual. With the knowledge of the line-strength, gas pressure, and line-shape function, the volume fraction of N₂O can be determined from the measured absorption coefficient at 2207.62 cm⁻¹ (see Supplementary information Section 2). Figure 5(b) compares the CRDS-determined volume fractions, ranging from 1 to 10 ppb, with the nominal values determined by the mixing ratio. The high degree of linearity in the fit, with an R-square value over 0.999, illustrates the accurate response of the spectrometer to N₂O measurements. Considering the Allan deviation analysis shown in Fig. 4(b), the minimum detection limit of the spectrometer is evaluated to be 1.9 \times 10⁻⁹ cm⁻¹ in absorption coefficient and 20 ppt in N₂O concentration at atmospheric pressure.

Conclusion

In conclusion, our research demonstrates that moderate optical feedback to a QCL enables agile and low-noise CRDS. By employing an AOM to split the QCL beam into two paths, we used the zero-order beam for optical feedback and directed the first-order diffraction to the optical cavity for ringdown measurements. Without using any active phase control of the reflected light, we demonstrated a considerable reduction in linewidth using moderate optical feedback (-18.2 dB). We verified

the effectiveness of the spectrometer by resolving a mid-infrared absorption line of ppb-level N₂O with a high SNR. Considering the similar behavior of ICLs³⁵, this approach can extend to ICLs with relatively low emission power. We also remark that this approach can be applied to other cavity-enhanced spectroscopic techniques beyond CRDS. Leveraging the narrowed QCL linewidth, we can mitigate laser-cavity locking noise, enhancing the detection limit of mid-infrared cavity-enhanced absorption spectroscopy (CEAS) and noise-immune cavity-enhanced optical heterodyne molecular spectroscopy (NICE-OHMS)^{36,37}. Additionally, the increased laser-cavity coupling efficiency results in higher intracavity power, making it promising for techniques such as cavity-enhanced photoacoustic spectroscopy and photothermal spectroscopy^{38,39}. Furthermore, the development of the QCL frequency comb allows for the use of optical feedback to potentially enhance frequency stability^{40,41}. Hence, we envision widespread adoption of this novel spectroscopic approach across various fields that demand highly sensitive, accurate, simplified and compact systems for chemical analysis.

References

- O'Keefe A, Deacon DAG. Cavity ring-down optical spectrometer for absorption measurements using pulsed laser sources. *Rev Sci Instrum* **59**, 2544–2551 (1988).
- Romanini D, Kachanov AA, Sadeghi N et al. CW cavity ring down spectroscopy. *Chem Phys Lett* **264**, 316–322 (1997).
- Berden G, Peeters R, Meijer G. Cavity ring-down spectroscopy: experimental schemes and applications. *Int Rev Phys Chem* **19**, 565–607 (2000).

4. Truong GW, Douglass KO, Maxwell SE et al. Frequency-agile, rapid scanning spectroscopy. *Nat Photonics* 7, 532–534 (2013).
5. Giusfredi G, Bartalini S, Borri S et al. Saturated-absorption cavity ring-down spectroscopy. *Phys Rev Lett* 104, 110801 (2010).
6. Gagliardi G, Loock HP. *Cavity-Enhanced Spectroscopy and Sensing* (Springer, Berlin Heidelberg, 2014).
7. Goldenstein CS, Spearrin RM, Jeffries JB et al. Infrared laser-absorption sensing for combustion gases. *Prog Energy Combust Sci* 60, 132–176 (2017).
8. Farooq A, Alquaity ABS, Raza M et al. Laser sensors for energy systems and process industries: perspectives and directions. *Prog Energy Combust Sci* 91, 100997 (2022).
9. Chen Q, Liang L, Zheng QL et al. On-chip readout plasmonic mid-IR gas sensor. *Opto-Electron Adv* 3, 190040 (2020).
10. Liu YH, Qiao SD, Fang C et al. A highly sensitive LITES sensor based on a multi-pass cell with dense spot pattern and a novel quartz tuning fork with low frequency. *Opto-Electron Adv* 7, 230230 (2024).
11. Mondelain D, Vasilchenko S, Čermák P et al. The self- and foreign-absorption continua of water vapor by cavity ring-down spectroscopy near 2.35 μm . *Phys Chem Chem Phys* 17, 17762–17770 (2015).
12. Vogler DE, Sigrist MW. Near-infrared laser based cavity ring-down spectroscopy for applications in petrochemical industry. *Appl Phys B* 85, 349–354 (2006).
13. Galli I, Bartalini S, Ballerini R et al. Spectroscopic detection of radiocarbon dioxide at parts-per-quadrillion sensitivity. *Optica* 3, 385–388 (2016).
14. McCart AD, Jiang J. Room-temperature optical detection of $^{14}\text{CO}_2$ below the natural abundance with two-color cavity ring-down spectroscopy. *ACS Sens* 7, 3258–3264 (2022).
15. Chen Y, Lehmann KK, Kessler J et al. Measurement of the $^{13}\text{C}/^{12}\text{C}$ of atmospheric CH_4 using near-infrared (NIR) cavity ring-down spectroscopy. *Anal Chem* 85, 11250–11257 (2013).
16. Cone MT, Mason JD, Figueroa E et al. Measuring the absorption coefficient of biological materials using integrating cavity ring-down spectroscopy. *Optica* 2, 162–168 (2015).
17. Long DA, Fleisher AJ, Liu Q et al. Ultra-sensitive cavity ring-down spectroscopy in the mid-infrared spectral region. *Opt Lett* 41, 1612–1615 (2016).
18. Baran SG, Hancock G, Peverall R et al. Optical feedback cavity enhanced absorption spectroscopy with diode lasers. *Analyst* 134, 243–249 (2009).
19. Argence B, Chanteau B, Lopez O et al. Quantum cascade laser frequency stabilization at the sub-Hz level. *Nat Photonics* 9, 456–460 (2015).
20. Zhao G, Tian JF, Hodges JT et al. Frequency stabilization of a quantum cascade laser by weak resonant feedback from a Fabry-Perot cavity. *Opt Lett* 46, 3057–3060 (2021).
21. Ohtsubo J. *Semiconductor Lasers: Stability, Instability and Chaos* 3rd ed (Springer, New York, 2013).
22. Schunk N, Petermann K. Numerical analysis of the feedback regimes for a single-mode semiconductor laser with external feedback. *IEEE J Quantum Electron* 24, 1242–1247 (1988).
23. Morville J, Kassi S, Chenevier M et al. Fast, low-noise, mode-by-mode, cavity-enhanced absorption spectroscopy by diode-laser self-locking. *Appl Phys B* 80, 1027–1038 (2005).
24. Kassi S, Stoltmann T, Casado M et al. Lamb dip CRDS of highly saturated transitions of water near 1.4 μm . *J Chem Phys* 148, 054201 (2018).
25. Burkart J, Romanini D, Kassi S. Optical feedback frequency stabilized cavity ring-down spectroscopy. *Opt Lett* 39, 4695–4698 (2014).
26. Zhao G, Bailey DM, Fleisher AJ et al. Doppler-free two-photon cavity ring-down spectroscopy of a nitrous oxide (N_2O) vibrational overtone transition. *Phys Rev A* 101, 062509 (2020).
27. Motto-Ros V, Morville J, Rairoux P. Mode-by-mode optical feedback: cavity ringdown spectroscopy. *Appl Phys B* 87, 531–538 (2007).
28. Maity A, Maithani S, Pradhan M. Cavity ring-down spectroscopy: recent technological advancements, techniques, and applications. *Anal Chem* 93, 388–416 (2021).
29. Coldren LA, Corzine SW, Mašanović ML. Dynamic effects. In Coldren LA, Corzine SW, Mašanović ML. *Diode Lasers and Photonic Integrated Circuits* (John Wiley & Sons, Inc., Hoboken, USA, 2012).
30. Capasso F, Gmachl C, Sivco DL et al. Quantum cascade lasers. *Phys Today* 55, 34–40 (2002).
31. Mezzapesa FP, Columbo LL, Brambilla M et al. Intrinsic stability of quantum cascade lasers against optical feedback. *Opt Express* 21, 13748–13757 (2013).
32. Zhao BB, Wang XG, Wang C. Strong optical feedback stabilized quantum cascade laser. *ACS Photonics* 7, 1255–1261 (2020).
33. Orr BJ, He YB. Rapidly swept continuous-wave cavity-ringdown spectroscopy. *Chem Phys Lett* 512, 1–20 (2011).
34. Truong GW, Perner LW, Bailey DM et al. Mid-infrared supermirrors with finesse exceeding 400000. *Nat Commun* 14, 7846 (2023).
35. Li XY, Fan ZF, Deng Y et al. 30-kHz linewidth interband cascade laser with optical feedback. *Appl Phys Lett* 120, 171109 (2022).
36. Yang M, Wang Z, Nie QX et al. Mid-infrared cavity-enhanced absorption sensor for ppb-level N_2O detection using an injection-current-modulated quantum cascade laser. *Opt Express* 29, 41634–41642 (2021).
37. Foltynowicz A, Schmidt FM, Ma W et al. Noise-immune cavity-enhanced optical heterodyne molecular spectroscopy: Current status and future potential. *Appl Phys B* 92, 313–326 (2008).
38. Nie QX, Wang Z, Borri S et al. Mid-infrared swept cavity-enhanced photoacoustic spectroscopy using a quartz tuning fork. *Appl Phys Lett* 123, 054102 (2023).
39. Jin W, Cao YC, Yang F et al. Ultra-sensitive all-fibre photothermal spectroscopy with large dynamic range. *Nat Commun* 6, 6767 (2015).
40. Liao XY, Wang XG, Zhou K et al. Terahertz quantum cascade laser frequency combs with optical feedback. *Opt Express* 30, 35937–35950 (2022).
41. Guan W, Li ZP, Wu SM et al. Relative phase locking of a terahertz laser system configured with a frequency comb and a single-mode laser. *Adv Photonics Nexus* 2, 026006 (2023).

Acknowledgements

This research was supported by National Natural Science Foundation of China (NSFC) (52122003, 62305279), China; Innovation and Technology Fund (GHP/129/20SZ) from the Innovation and Technology Commission, Hong Kong SAR, China; Collaborative Research Fund (C4002-22Y) and General Research Fund (14208221) from the University Grants Committee, Hong Kong SAR, China.

Author contributions

W. Ren proposed the original idea of the project. W. Ren supervised the project. Q. X. Nie designed and built the experimental setup. Q. X. Nie, Y. B. Peng and Q. H. Chen conducted the experiment and collected the data. Q. X. Nie conducted the data analysis. N. W. Liu, C. Wang and Z. Wang contributed to the discussion of the research. Q. X. Nie wrote the manuscript. W. Ren and C. Wang edited the manuscript.

Competing interests

The authors declare no competing financial interests.

Supplementary information

Supplementary information for this paper is available at <https://doi.org/10.29026/oea.2024.240077>



Scan for Article PDF